Proceedings of the Sixth International Conference on
Railway Technology: Research, Development and Maintenance
Edited by: J. Pombo
Civil-Comp Conferences, Volume 7, Paper 9.5
Civil-Comp Press, Edinburgh, United Kingdom, 2024
ISSN: 2753-3239, doi: 10.4203/ccc.7.9.5
©Civil-Comp Ltd, Edinburgh, UK, 2024

Optimizing Wear Prediction Models for High-Speed Railway: A Numerical Sensitivity Analysis

Z. Shi[1], E. Meli[1], Y. Sun[2] and A. Rindi[1]

[1]Department of Industrial Engineering of Florence (DIEF), University of Florence, Italy
[2]College of Transportation Science and Engineering, Nanjing Tech University, China

Abstract

The modelling for wear profile prediction has been one of the most fundamental tasks in railway engineering science. This paper presents a numerical sensitivity study of a wear prediction model for a high-speed railway application. It firstly introduces the wear prediction model including a vehicle-track coupled model for vehicle dynamical simulation, the local contact model for wheel-rail interaction, and an energetic approach for surface wear evaluation. Afterwards, the parameter setting of the current wear prediction model is presented, consisting of 3 factors, the discretization size of wheel-rail contact patch, the smoothing algorithm, and the depth threshold of each updating step. The results show that, first of all, the influence of patch discretization size is dominating, that in some cases when the friction coefficient is rather high, the determination of the slip can be skipped when choosing an improper value of mesh size. In those cases, the suggested mesh size could be deficient in the cases of high friction coefficient. Secondly, the variation of smoothing algorithms makes a difference in the wear depth evolution, but the influence is slight. Thirdly, the influence of the depth threshold is remarkable on both the efficiency and the accuracy. A trade-off between accuracy and efficiency should be balanced at the specific task.

Keywords: Chinese high-speed railway, wheel wear, numerical analysis, sensitivity analysis, mesh size, smoothing.

1 Introduction

Wear at wheel-rail contact interface alters the profiles for both rail and wheel over time, influences the interaction of wheel and rail instantaneously and further threatens the running performance of the vehicle and the service performance of the track in the long-

term run. It is regarded one of the most fundamental research in the railway engineering field.

In the past years, vehicle dynamics, contact mechanics, and tribology based research has intensively promoted the understanding of wear in wheel-rail contact and dynamic models to predict the evolution [1]. Braghin et al. [2,3] conducted early investigations on wear prediction for railway application, constituting a basic prototype for later research. Jin et al. [4] conducted wear investigations on rail and wheel, locomotive and passenger car, high speed and heavy haul railway lines [5-8]. This continuous, and systematic work is based on different tools, consists of different scenarios. Pombo et al. established a computational tool that is able to predict the evolution of the wheel profiles, and conducted comparative study [9,10]. Sun et al. [11] developed a wear prediction tool to study the relations between wear and other parameters, such as the influence of track random irregularity on rail non-uniform wear and the effect of hollow-worn wheels on the evolution of rail wear [11[11],12]. Other participating investigations on different types of vehicles, railway lines, wheel profiles, and rail profiles in the context of wheel-rail wear prediction can be found prosperously in [13-16]. To predict the wear evolution between the wheel-rail interface, a general methodology is demanded to include a dynamics model, a local contact model, a wear evaluation model, and a profile updating strategy, shown in Figure 1. In practice, different sub-parts are applied for a wide range of various investigations. For instance, there are four representative wear models among researchers up to now, BRR (British Rail Research) model, Zobory model, USFD (University of Sheffield) model, and KTH model [17~20]. There are several publications investigating the comparison of different applications, such as De Arizon et al. [21] compared KTH model, Zobory model, and BBR model for a tramway condition, Pombo et al. [10] compared the BRR, KTH, USFD models for a urban railway condition with very sharp curves, and Peng et al. [22] has discussed BBR, Zobory, KTH, USFD models adapted them for wheel polygonization study in a tangential track and high-axle-load locomotive scenario. These studies are helpful in clarifying the differences between different subparts. Figure 1 shows a general methodology for the wear prediction model that has been widely used by researchers. Many parameter settings are usually included in this integrated scheme. Each part of the scheme (shown in Figure 1) may affect the accuracy and efficiency of the prediction model. However, an observation on how various factors comparatively affecting the wear prediction model has not yet been sufficiently addressed. A numerical sensitivity analysis could reveal the accuracy and the robustness of this kind of wear models. Therefore, it would be meaningful to systematically discuss the sensitivity analysis of the wear prediction models from a numerical point of view.

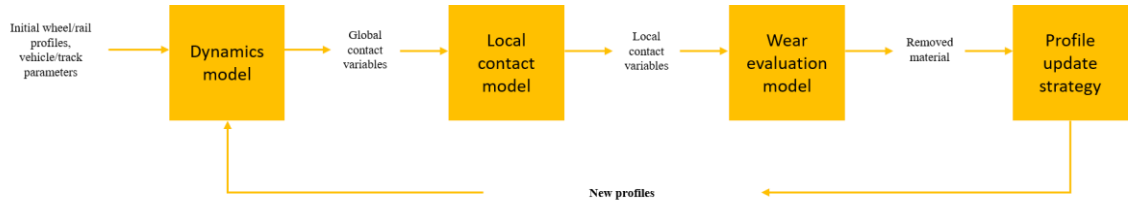

Figure 1: A general methodology for the wear prediction model.

In previous study, the authors have developed a wear prediction tool and have used the tool for several applications [23~31]. In papers [23-24,27], a model consisting of two interactive parts was developed, vehicle model part for dynamical analysis and damage model part for wear estimation. Based on the wear model, the group has developed innovative wheel profiles to reduce the wear of the wheel [25,26] and improved the

accuracy and efficiency [28,29]. Simulated results have shown the optimisation is effective to improve the wheel wear condition. After that, innovations are achieved in papers [30] and [31], which includes the consideration of more components and the track flexibility, which is necessary for higher frequency investigations. This paper firstly introduces a wear prediction model including a vehicle-track coupled model for vehicle dynamical simulation, the local contact model for wheel-rail interaction, and an energetic approach for surface wear evaluation. Secondly, we present the numerical sensitivity analysis of current wear model, based on a high-speed railway application. The sensitivity analysis will be addressed through 3 factors, the discretization size of wheel-rail contact patch, the smoothing algorithm, and the depth threshold of each updating step.

2 Modelling

This section firstly presents the architecture of the wear prediction model, then details the model with particular attention paid on the local contact model and profile update strategy, and finally introduces the parameter settings of sensitivity analysis.

2.1 Architecture of the model

The general architecture of the wear prediction model is shown in Figure 2. As it depicts, two main parts are included, the dynamics model and the wear model. Inside the dynamics model, kinematic variables, contact points and forces are transferred to the global contact model in order to obtain the contact variables. Based on the results from the dynamics model, the local contact variables can be calculated and then further passed to wear evaluation model. The wear evaluation model estimates the removed material from the profiles of the wheel and rail. After obtaining the removed material, the profiles are updated, generating new profiles, which become the new input profiles for vehicle-track coupled model.

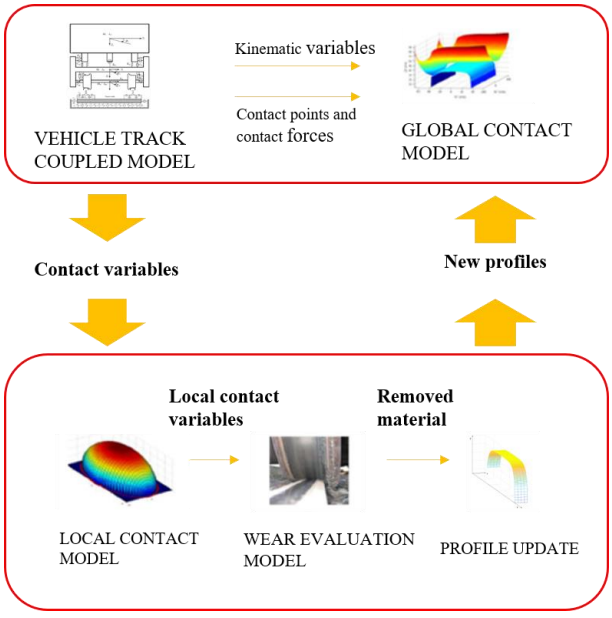

Figure 2: A general architecture of wear prediction model.

The dynamics model is based on the theory of vehicle-track coupled dynamics [32,33], which includes an MBS vehicle model, and a multi-layer track model. The wear calculation model is based on the energy transfer method, which assumes the material loss as a function of the energy dissipated at the contact patch, as referred in [3,30]. The integration of each part in Figure 2 can be referenced in [31,34].

2.2 Model details

This section gives the details of the model presented in Figure 2. After running the dynamical simulation for vehicle-track system, a local contact model is designed to calculate the local contact variables. A reference system is defined at the wheel-rail interface on the contact plane, shown in Figure 2, which illustrates the x, y and z axes being the longitudinal, the transversal and the normal directions of the contact area.
The semi-axes a and b of the elliptical patch are discretized in a bi-dimensional grid, where b is the transversal axis with respect to the motion direction, and a is the longitudinal axis along the motion direction (Shown in Figure 3). The grid resolution will be written as following:

$$\Delta y = \frac{2b}{n_y - 1} \tag{1}$$

In Eq. (1), the transversal axis is divided in equal $n_y - 1$ parts of magnitude Δy by means of n_y equidistant nodes. Since the discretion in the longitudinal axis is geometric dependent on the transversal axis, the discretion can be achieved by means of n_x equidistant nodes into $n_x - 1$ equal parts, as

$$\Delta x(y) = \frac{2a(y)}{n_x - 1} \tag{2}$$

$$a(y) = a\sqrt{1 - \frac{y^2}{b^2}} \tag{3}$$

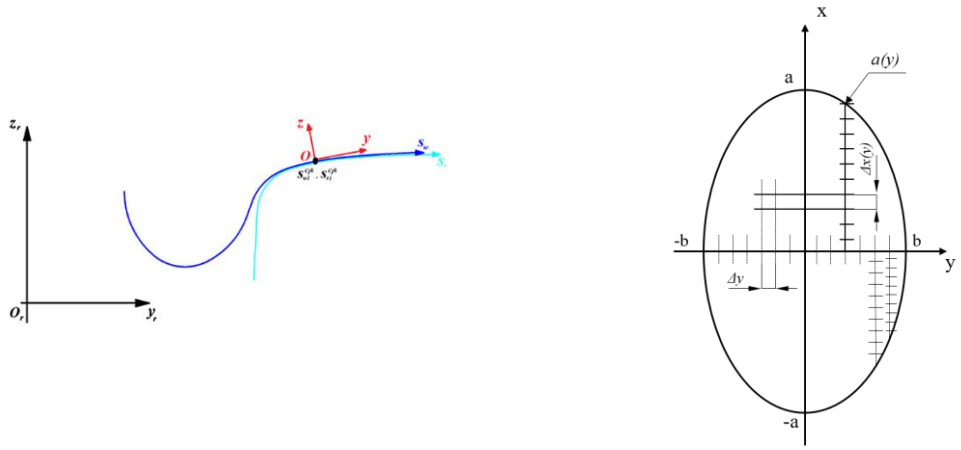

(a) x, y and z axes of the contact interface (b) Contact patch discretization

Figure 3: Reference system at the wheel-rail interface.

Inside the patch discretisation, we use the following equation to determine if the point (x_i, y_i) falls into the sliding area or the adhesion area:

if $\left\|\mathbf{p}_A(x_i,y_j)\right\| \le \mu(x_i,y_j)\,p_n(x_i,y_j)$

$$\begin{cases}\mathbf{p}_t(x_i,y_j)=\mathbf{p}_A(x_i,y_j)\\ \mathbf{s}(x_i,y_j)=0\end{cases} \tag{4}$$

if $\left\|\mathbf{p}_A(x_i,y_j)\right\| > \mu(x_i,y_j)\,p_n(x_i,y_j)$

$$\begin{cases}\mathbf{p}_t(x_i,y_j)=\mu(x_i,y_j)\,p_n(x_i,y_j)\mathbf{p}_A(x_i,y_j)/\left\|\mathbf{p}_A(x_i,y_j)\right\|\\ \mathbf{s}(x_i,y_j)=\dfrac{LV}{\Delta x(y_j)}\left[(\mathbf{p}_t(x_i,y_j)-\mathbf{p}_A(x_i,y_j)\right]\end{cases} \tag{5}$$

where μ(xi,yi) is the friction coefficient in (x_i,y_i), $\mathbf{p}_A(x_i,y_j)$ and $p_n(x_i,y_j)$ represent the adhesion pressure and normal pressure of (x_i,y_i) ,L and V are the flexibility coefficient and longitudinal vehicle speed, while $\mathbf{p}_t(x_i,y_j)$ and $\mathbf{s}(x_i,y_j)$ are the tangential pressure and sliding velocity in (x_i,y_i). The determination for corresponding parameters could be referenced in [30].

After we obtain the local contact parameters, it is possible to calculate the wear based on energy transfer method, which assumes the material loss as a function of the energy dissipated at the contact patch, as referred in [3], with the following equations:

$$I_w = \frac{T\gamma(x,y)}{A} = \frac{\overrightarrow{p_t}\cdot\vec{s}(x,y)}{V} \tag{6}$$

$$K_w(I_w)=\begin{cases}5.3I_w & I_w<10.4\\ 55.1 & 10.4\le I_w\le 77.2\\ 61.9I_w-4778.7 & I_w>77.2\end{cases} \tag{7}$$

where T and γ are creep force and creepage, I_w and $K_w(I_w)$ are wear index and wear rate, respectively. Given the wear rate from Eq.7, the volume of removed material on the wheel, for unit of distance travelled by the vehicle can be calculated as:

$$\delta^{jk}_{P_{wi}(t)}(x,y) = K_w\left(I^{jk}_{wi}\right)\frac{1}{\rho} \tag{8}$$

where $\delta^{jk}_{P_{wi}(t)}(x,y)$ represents the wear depth distributions for the the i th contact patch of the j th wheel during the k th of the total simulation conditions and ρ is the density of the material. After we obtain the amount of worn material for the profiles at each step, the result will be transferred as inputs for the next step in a loop strategy, so as to achieve an updated profile. The update strategy includes following operations:

- For each contact step, get the spatial integration of all the wear contributions inside the contact patch, along the longitudinal direction and then get the average value per unit length. In this procedure, we study the contact patch at each time step, and assume that the wear effect of contact at each time step on the wheel surface is equal.
- During a certain time series of simulation, sum all the wear contributions coming from all time-steps to obtain the depth of the removed material from the wheel. For one time point among the time series, sum the wear contributions coming from all the contact points of a contact pair.

- Amplify the removed material during the dynamic simulations to reduce the simulated track length through a scaling procedure.
- A smoothing procedure is adopted to remove the numerical noise.

With Eq. 8, the longitudinal integration at each contact point path can be written as:

$$\delta^{tot}_{P^{jk}_{wi}}(y)=\frac{1}{2\pi w_{y^{jk}_{wi}}}\int_{-a(y)}^{+a(y)}\delta_{P^{jk}_{wi}}(x,y)dx \tag{9}$$

where $\delta^{tot}_{P^{jk}_{wi}}(y)$ represents the accumulated wear distribution along x direction for the wheel, the $w_{y^{jk}_{wi}}$ is the radius of the wheel at y^{jk}_{wi}.

$$\begin{aligned}\Delta_{P^{jk}_{wi}}(y)&=\int_{T_{in}}^{T_{end}}\delta^{tot}_{P^{jk}_{wi}(t)}(y)V(t)\,dt\\&\approx\int_{T_{in}}^{T_{end}}\delta^{tot}_{P^{jk}_{wi}(t)}(s_w-s^{cjk}_{wi})V(t)\,dt=\Delta_{P^{jk}_{wi}}(s_w)\end{aligned} \tag{10}$$

The natural abscissa s_w of the curve $w(y_w)$ has been considered to better calculate the worn profiles. Afterwards, we sum all the contributions from each simulation time step by track integration, as

$$\sum_{i=1}^{N_{PDC}}\Delta_{P^{jk}_{wi}}(s_w)=\Delta_{P^{jk}_{w}}(s_w) \tag{11}$$

where N_{PDC} is the maximum number of contact points of each wheel-rail pair.

$$\sum_{k=1}^{N_c}p_k\sum_{j=1}^{N_w}\Delta_{P^{jk}_{w}}(s_w)=\overline{\Delta}_w(s_w) \tag{12}$$

where N_c is the number of the simulated railway curved segments, and N_w is the number of the wheelsets for the vehicle, p_k is the weighting factor of the kth curve derived from the statistical analysis.

Assuming that, inside each discrete unit, the wear quantity is close to linear with the travelled distance. This requires the unit length small enough to neglect the profile variation between two consequent units. In this way, the total length is discretized by a series of unit lengths, and each unit length is discretized by a series of track lengths. Mark the total mileage of the worn vehicle as total length km_{tot}, the unit length inside each discrete unit as km_{unit}, and the track length for each simulation inside one unit as l_{track}. Figure 4 illustrates the discretization of the total mileage. It is possible to amplify the removed material during the dynamic simulations by means of a scaling factor which increases the distance travelled by the vehicle.

Figure 4: Discretization of the total mileage.

An adaptive approach is applied for updating the profile:

$$\overline{\Delta}^{w}(s_w)\frac{km_{step}}{l_{track}}=\overline{\Delta}^{wsc}(s_w) \tag{13}$$

where km_{step} is calculated in an adaptive way setting a threshold value D_{step}^{w} on the maximum of the removed material quantity on the wheel at each discrete step:

$$km_{step} = l_{track} \frac{D_{step}^{w}}{\max\left(\overline{\Delta}_{j}^{w}\left(s_{w}\right)\right)} \tag{14}$$

where $\max\left(\overline{\Delta}_{j}^{w}\left(s_{w}\right)\right)$ corresponds to the maximum value of wear depth obtained from the simulation before the scaling operation.

The smoothing of the removed material function is necessary to remove the numerical noise that affects this quantity and that would be passed to the new profile of wheel and rail causing problems to the global contact model, as the following equation:

$$\Gamma\left[\overline{\Delta}^{wsc}\left(s_{w}\right)\right] = \overline{\Delta}_{sm}^{wsc}\left(s_{w}\right) \tag{15}$$

where $\overline{\Delta}^{wsc}\left(s_{w}\right)$ and $\overline{\Delta}_{sm}^{wsc}\left(s_{w}\right)$ represent the removed material quantity on the wheel, before and after smoothing.

2.3 Parameter settings of sensitivity analysis

The accuracy and efficiency are always two key factors to evaluate a model. In the context of wheel-rail and vehicle-track interaction models, many numerical parameter settings would be touched upon. In this article, we address the sensitivity analysis through 3 factors, the discretization size of wheel-rail contact patch, the smoothing algorithm, and the depth threshold of each updating step. The mesh size for patch discretisation refers to Equations (1) and (2), smoothing algorithm refers to Equation (15), and the depth threshold for updating refers to Equation (14) in Section 2.2. We present the numerical sensitivity analysis of current wear model, based on a high-speed railway application, including the CRH2 EMU vehicle and the CRTS I slab track, where the maximum running speed is 350 km/h. The types of the wheel and the rail profile in this case are the standard LMA and CN60 profiles. Parameters of the CRH2 high speed vehicle and the slab track can be referred in [35]. To investigate the effect of mesh size on the wear prediction model thoroughly, we have set a group of size numbers, from 21×21 to 301×301. The smoothing algorithm and updating step-length are involved in the profile updating strategy. During this procedure, the choice of smoothing algorithm may vary. There are several choices used, for instance, the wavelet filtering method [13], the moving average method [11], and the cubic spline smoothing method [7]. As for the updating step-length, we study different values under 0.05mm, 0.1mm and 0.2mm. The settings of discretization size, smoothing algorithm and updating step-length for sensitivity analysis are shown in Table 1.

Discretization size		
21×21	…	301×301
Smoothing algorithm		
Wavelet filtering method	Moving average method	Cubic spline smoothing method
Updating step-length		
D_{step}^{w} =0.2mm	D_{step}^{w} =0.1mm	D_{step}^{w} =0.05mm

Table 1: Sensitivity analysis settings of discretization size, smoothing algorithm and updating step-length.

3 Results and discussion

To conduct the numerical sensitivity analysis of the model, we considered a general simulation condition to reach a high efficiency, that the vehicle passing by a railway track at a speed of 250 km/h, and the track layout considers a 6000 m radius curve segment. The parameters of the vehicle-track system are presented in reference [35]. To analyse the discretization size, the travelling distance is taken as the indicator for comparing the numerical accuracy, which can represent the wear ratio of the wheel. At the discussions of smoothing algorithm and depth threshold, the indicator for comparing the numerical accuracy is represented by wear depth of a wheel.

3.1 Discretization size

From Eqs. (1) ~ (4), it is seen that the mesh refinement determines if slip zone is found inside the current contact patch, and further participate the wear calculation. At the meantime, the friction coefficient brings conditional restriction. Therefore, cases with different friction coefficient (0.05~0.4) are simulated. At the investigation of mesh size setting, we consider one step of update, and threshold value of each step is set as 0.1 mm. The cubic spline smoothing method is adopted for smoothing. The results of calculated travelling distance after the first step are shown in Table 2. The percentage change of travelling distance is shown in Table 3.

Distance [km]	**mu=0.4**	**mu=0.35**	**mu=0.3**	**mu=0.25**	**mu=0.2**	**mu=0.15**	**mu=0.1**	**mu=0.05**
21×21	*	*	*	*	*	1.57E+05	2.35E+04	1.57E+04
41×41	*	*	*	2.27E+07	7.20E+04	2.39E+04	1.52E+04	1.38E+04
61×61	*	*	8.49E+06	8.01E+04	2.82E+04	1.73E+04	1.33E+04	1.33E+04
81×81	*	1.07E+07	1.12E+05	3.50E+04	2.07E+04	1.50E+04	1.25E+04	1.30E+04
101×101	2.83E+07	2.23E+05	4.79E+04	2.54E+04	1.75E+04	1.38E+04	1.20E+04	1.28E+04
121×121	2.12E+06	7.05E+04	3.21E+04	2.11E+04	1.58E+04	1.30E+04	1.17E+04	1.27E+04
141×141	1.18E+05	4.38E+04	2.61E+04	1.87E+04	1.47E+04	1.25E+04	1.15E+04	1.26E+04
161×161	6.47E+04	3.30E+04	2.24E+04	1.70E+04	1.40E+04	1.22E+04	1.14E+04	1.26E+04
181×181	4.53E+04	2.78E+04	2.02E+04	1.60E+04	1.34E+04	1.19E+04	1.12E+04	1.25E+04
201×201	3.55E+04	2.44E+04	1.87E+04	1.52E+04	1.30E+04	1.17E+04	1.11E+04	1.25E+04
221×221	3.02E+04	2.20E+04	1.74E+04	1.45E+04	1.27E+04	1.15E+04	1.10E+04	1.24E+04
241×241	2.70E+04	2.04E+04	1.65E+04	1.41E+04	1.24E+04	1.14E+04	1.10E+04	1.24E+04
261×261	2.44E+04	1.92E+04	1.58E+04	1.37E+04	1.22E+04	1.13E+04	1.09E+04	1.24E+04
281×281	2.25E+04	1.82E+04	1.53E+04	1.33E+04	1.20E+04	1.12E+04	1.09E+04	1.24E+04
301×301	2.11E+04	1.73E+04	1.48E+04	1.30E+04	1.18E+04	1.11E+04	1.08E+04	1.23E+04

*Note: [*] refers to a maximum value beyond the calculation range.

Table 2: Influence of mesh size on numerical accuracy: travelling distance.

Distance [km]	**mu=0.4**	**mu=0.35**	**mu=0.3**	**mu=0.25**	**mu=0.2**	**mu=0.15**	**mu=0.1**	**mu=0.05**
41×41	*	*	*	*	*	-85%	-36%	-12%
61×61	*	*	*	*	*	-28%	-12%	-4%
81×81	*	*	*	-56%	-27%	-13%	-6%	-2%

101×101	*	*	-57%	-27%	-15%	-8%	-4%	-1%
121×121	*	-68%	-33%	-17%	-10%	-5%	-3%	-1%
141×141	-94%	-38%	-19%	-11%	-7%	-4%	-2%	-1%
161×161	-45%	-25%	-14%	-9%	-5%	-3%	-1%	0%
181×181	-30%	-16%	-10%	-6%	-4%	-2%	-1%	0%
201×201	-22%	-12%	-8%	-5%	-3%	-2%	-1%	0%
221×221	-15%	-10%	-7%	-4%	-2%	-1%	-1%	0%
241×241	-11%	-7%	-5%	-3%	-2%	-1%	-1%	0%
261×261	-10%	-6%	-4%	-3%	-2%	-1%	-1%	0%
281×281	-8%	-5%	-3%	-2%	-2%	-1%	0%	0%
301×301	-6%	-5%	-3%	-2%	-1%	-1%	0%	0%

*Note: [*] refers to a maximum value beyond the calculation range.

Table 3: Influence of different mesh size on numerical accuracy: Percentage change of travelling distance.

Each row of the Table 1 informs that, at current discretized size, the distance value changes as friction coefficient differs. And each column of the table indicates how the distance value changes as mesh size differs, at current friction coefficient. Taking the third column of Table 2 as an example, here gives the analysis in the case of the friction coefficient being 0.35. If the discretized size is rougher than *61×61*, the local contact model calculates a rather great value. As it is assumed that the wear occurs only in the slip region of the contact patch, the great value reveals that no slip is captured by the local contact model, referring Eq. 4. If the discretized size is finer than *61×61*, the slip is considered, however, as the patch becomes more finely discretized, the result tends to a stable value. This indicates that the mesh size of the grid affects the accuracy of the wear prediction model, by the local contact model. Meanwhile, take the third row as an example, here presents the analysis for the case of the patch grid mesh being *61×61*, the case of the fourth row. It is seen that, for the cases that the friction coefficients are higher than 0.35, no slip is captured by the model, and if the friction coefficient is lower than 0.3, the travelling distance decreases, which means the slip area is greater and the worn material is more.

Previous studies usually take a certain value, for example *41×41*, as a suggested mesh size, and it is sufficient at low friction coefficient. But in some cases when the friction coefficient is rather high, the determination of the slip can be skipped. In those cases, the suggested mesh size could be deficient in the cases of high friction coefficient. To understand the requirements of the grid mesh at different cases, the percentage change is calculated based on the values of the travelling distance, shown in Table 3. Besides, the influence of mesh size on calculating efficiency is remarkable in the wear evaluation step as the calculation time depends on the number of iterations. However, from the view of global model, the wear evaluation model cost much less time on comparing with the dynamics model. Therefore, it is suggested to increase the mesh size as high as necessary. For a certain friction coefficient, a tendency is seen that the relative change develops to zero as the mesh size gets larger. To obtain a high accuracy by using the proposed wear prediction model, it is necessary to discretize the contact patch with an adequate mesh. It is obvious that, at different friction coefficient, the mesh size should meet different requirements. Note that, the Tables 2 and 3 represent the results only for current simulating condition, that the vehicle passing by 6000 m radius curve at a speed of 250 km/h.

3.2 Smoothing algorithm

To understand the effect of different smoothing algorithms, we have set up the simulation of predicting the wear of a railway curve segment the same as Section 3.1. The evolutions of the wear depth by three different inputs are compared: the wavelet filtering method (Case 1), the moving average method (Case 2), and the cubic spline smoothing method (Case 3). During the simulation, the friction coefficient between the wheel and the rail is set as 0.3, and the discretization size is set as 201×201. Eight steps of updating are considered, with threshold value of each step being set as 0.1 mm. The results are illustrated in Figure 5.

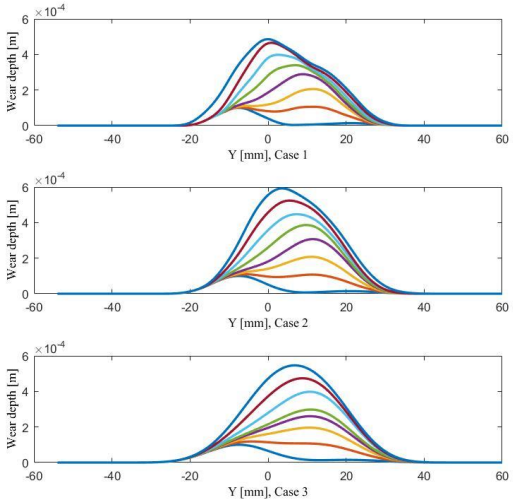

Figure 5: Wear depth evolution with different smoothing algorithms.

It is seen from Figure 5 that the variation of smoothing algorithms makes a difference on the wear depth evolution, but the influence is slight. In Cases 1-3, the resulted first step is found very close. As the update times rise, the difference becomes more obvious, for example in Step 4 and 5. But after that the wear depth evolution becomes similar again. The running distance with different smoothing algorithms is shown in Figure 6. It is found with similar trends, that the influence of smoothing algorithm is slight.
Besides, it is found that the influence of smoothing algorithm on calculating efficiency is not obvious.

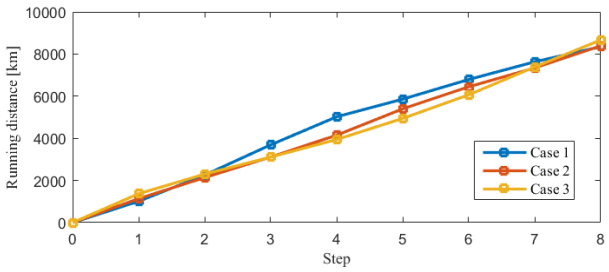

Figure 6: Running distance with different smoothing algorithms.

3.3 Updating step-length

To understand the influence of depth threshold on wheel wear evolution, we have set up the simulation of predicting the wear of similar scenario as described in Section 2.3. We have compared the evolution of the wear depth by three different inputs: D_{step}^{w} =0.2 mm

(Case 1), D^{w}_{step} =0.1 mm (Case 2), and D^{w}_{step} =0.05 mm (Case 3). To calibrate the wear depth, we have set up 4 steps, 8 steps, and 16 steps for different cases, so that every simulation consider the wear evolution in a close range. The results are illustrated in Figure 7.

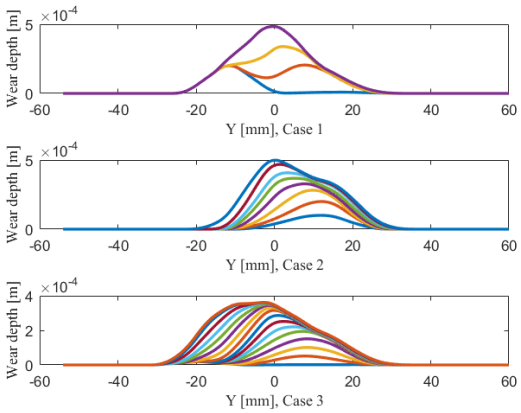

Figure 7: Wear depth evolution with different depth thresholds.

It is seen from Figure 7 that at the first step, Case 1 is found with obvious difference with the other two cases, which are supposed to be of higher accuracy. This implies that 0.2 mm as the depth threshold is an over-length threshold. Combining all the steps considered for three cases, we find that even the final evolution results show similarity, a huge difference appears during the development process. As the prediction of wear is strongly related to the process, it could be concluded that the case D^{w}_{step} =0.2 mm is not well chosen. The running distance with different updating step-length is shown in Figure 8.

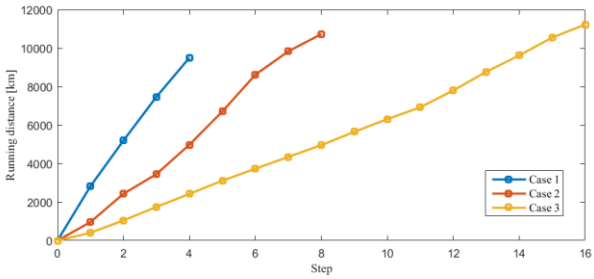

Figure 8: Running distance with different updating step-lengths.

It is seen from Figure 8 that, within the considered wear depth, three different updating step-length leads to values of total running distance close to each other. On the other hand, the depth threshold is linearly related to the calculating efforts. In this discussion, the Case 3 demands twice as long as the Case 2, and fours times as long as Case 1.

3.4 Discussion

Above results have presented an overview of the numerical sensitivity analysis of the considered wear model for the current railway application. Concerning the discretization size, we have reached a final convergence as expected. The results show that the influence of patch discretization size is dominating, that in some cases when the friction coefficient is rather high, the determination of the slip can be skipped when choosing an improper value of mesh size. In those cases, the suggested mesh size could be deficient in the cases of high friction coefficient. Concerning the smoothing algorithm and the updating step-

length, the model shows robustness against a change of the considered parameters. The variation of smoothing algorithms makes a difference in the wear depth evolution, but the influence is slight. The influence of the depth threshold is remarkable on both the efficiency and the accuracy.

4 Conclusions and Contributions

In this paper, the numerical sensitivity analysis of a wear prediction model based on a high-speed railway line is presented by 3 factors, the discretization size, the smoothing algorithm, and the updating step-length. Main conclusions can be drawn in the following:
(1) The influence of discretization size is dominating on accuracy. A proper discretization size could be depended on the corresponding friction coefficient between the wheel and the rail. A final convergence concerning the influence of discretization size has been found through the numerical sensitivity analysis.
(2) The variation of smoothing algorithms makes a difference on the wear depth evolution, but the influence is slight. The model shows robustness against a change of the considered parameters.
(3) The influence of the depth threshold is remarkable on both the efficiency and the accuracy. And a trade-off between the accuracy and efficiency will suggest in those cases a choice of 0.1 mm (Case 2).
It should be noted that in this paper, the results are based on one representative situation to simulate the wear prediction. In future developments, a general numerical analysis could be extended through including more prediction models, with respect to different contact models, and wear evaluation models under different conditions.

References

[1] Tao, G., Wen, Z., Jin, X. et al. Polygonisation of railway wheels: a critical review. Rail. Eng. Science 28, 317–345 (2020).

[2] Braghin, F., Bruni, S. & Resta, F. (2002) Wear of Railway Wheel Profiles: A Comparison between Experimental Results and a Mathematical Model, Vehicle System Dynamics, 37:sup1, 478-489,

[3] Braghin, F., Lewis, R., Dwyer-Joyce, R. S., & Bruni, S. (2006). A mathematical model to predict railway wheel profile evolution due to wear. Wear, 261(11-12), 1253-1264.

[4] Jin, X., Wen, Z., Xiao, X. et al. A numerical method for prediction of curved rail wear. Multibody Syst Dyn 18, 531–557 (2007).

[5] Li, X., Jin, X., Wen, Z., Cui, D., & Zhang, W. (2011). A new integrated model to predict wheel profile evolution due to wear. Wear, 271(1-2), 227-237.

[6] Li, X., Yang, T., Zhang, J., Cao, Y., Wen, Z., & Jin, X. (2016). Rail wear on the curve of a heavy haul line—Numerical simulations and comparison with field measurements. Wear, 366, 131-138.

[7] Tao, G. Q., Du, X., Zhang, H. J., Wen, Z. F., Jin, X. S., & Cui, D. B. (2017). Development and validation of a model for predicting wheel wear in high-speed trains. Journal of Zhejiang University-SCIENCE A, 18(8), 603-616.

[8] Tao, G., Wen, Z., Guan, Q., Zhao, X., Luo, Y., & Jin, X. (2019). Locomotive wheel wear simulation in complex environment of wheel-rail interface. Wear, 430, 214-221.

[9] Pombo, J., Ambrósio, J., Pereira, M. et al. A study on wear evaluation of railway wheels based on multibody dynamics and wear computation. Multibody Syst Dyn 24, 347–366 (2010).
[10] Pombo, J., Ambrosio, J., Pereira, M., Lewis, R., Dwyer-Joyce, R., Ariaudo, C., & Kuka, N. (2011). Development of a wear prediction tool for steel railway wheels using three alternative wear functions. Wear, 271(1-2), 238-245.
[11] Sun, Y., Guo, Y., & Zhai, W. (2019). Prediction of rail non-uniform wear–Influence of track random irregularity. Wear, 420, 235-244.
[12] Sun, Y., Guo, Y., Lv, K., Chen, M., & Zhai, W. (2019). Effect of hollow-worn wheels on the evolution of rail wear. Wear, 436, 203032.
[13] Ding, J., Li, F., Huang, Y., Sun, S., & Zhang, L. (2014). Application of the semi-Hertzian method to the prediction of wheel wear in heavy haul freight car. Wear, 314(1-2), 104-110.
[14] Luo, R., Shi, H., Teng, W., & Song, C. (2017). Prediction of wheel profile wear and vehicle dynamics evolution considering stochastic parameters for high-speed train. Wear, 392, 126-138.
[15] Li, Y., Ren, Z., Enblom, R., Stichel, S., & Li, G. (2020). Wheel wear prediction on a high-speed train in China. Vehicle System Dynamics, 58(12), 1839-1858.
[16] Ye, Y., Sun, Y., Dongfang, S. et al. Optimizing wheel profiles and suspensions for railway vehicles operating on specific lines to reduce wheel wear: a case study. Multibody Syst Dyn 51, 91–122 (2021).
[17] Pearce, T. G., & Sherratt, N. D. (1991). Prediction of wheel profile wear. Wear, 144(1-2), 343-351.
[18] Zobory, I. (1997). Prediction of wheel/rail profile wear. Vehicle System Dynamics, 28(2-3), 221-259.
[19] Lewis, R., & Olofsson, U. (2004). Mapping rail wear regimes and transitions. Wear, 257(7-8), 721-729.
[20] Jendel, T. (2002). Prediction of wheel profile wear—comparisons with field measurements. Wear, 253(1-2), 89-99.
[21] De Arizon, J., Verlinden, O., & Dehombreux, P. (2007). Prediction of wheel wear in urban railway transport: comparison of existing models. Vehicle System Dynamics, 45(9), 849-866.
[22] Peng, B., Iwnicki, S., Shackleton, P., & Crosbee, D. (2019). Comparison of wear models for simulation of railway wheel polygonization. Wear, 436, 203010.
[23] Ignesti, M., Malvezzi, M., Marini, L., Meli, E., & Rindi, A. (2012). Development of a wear model for the prediction of wheel and rail profile evolution in railway systems. Wear, 284, 1-17.
[24] Ignesti, M., Marini, L., Meli, E., & Rindi, A. (2012). Development of a model for the prediction of wheel and rail wear in the railway field. Journal of computational and nonlinear dynamics, 7(4).
[25] Ignesti, M., Innocenti, A., Marini, L., Meli, E., & Rindi, A. (2013). Development of a wear model for the wheel profile optimisation on railway vehicles. Vehicle system dynamics, 51(9), 1363-1402.
[26] Ignesti, M., Innocenti, A., Marini, L., Meli, E., Rindi, A., & Toni, P. (2013). Wheel profile optimization on railway vehicles from the wear viewpoint. International Journal of Non-Linear Mechanics, 53, 41-54.
[27] Ignesti, M., Innocenti, A., Marini, L., Meli, E., & Rindi, A. (2014). Development of a model for the simultaneous analysis of wheel and rail wear in railway systems. Multibody System Dynamics, 31(2), 191-240.

[28] Innocenti, A., Marini, L., Meli, E., Pallini, G., & Rindi, A. (2014). Development of a wear model for the analysis of complex railway networks. Wear, 309(1-2), 174-191.
[29] Innocenti, A., Marini, L., Meli, E., Pallini, G., & Rindi, A. (2014). Prediction of wheel and rail profile wear on complex railway networks. International Journal of Rail Transportation, 2(2), 111-145.
[30] Butini, E., Marini, L., Meacci, M., Meli, E., Rindi, A., Zhao, X. J., & Wang, W. J. (2019). An innovative model for the prediction of wheel-Rail wear and rolling contact fatigue. Wear, 436, 203025.
[31] Shi, Z., Zhu, S., Rindi, A., & Meli, E. (2021). Development and validation of a wear prediction model for railway applications including track flexibility. Wear, 486, 204092.
[32] Zhai, W. (2020). Vehicle–track coupled dynamics: theory and applications. Springer Nature.
[33] Zhai, W., Wang, K., & Cai, C. (2009). Fundamentals of vehicle–track coupled dynamics. Vehicle System Dynamics, 47(11), 1349-1376.
[34] Shi, Z., Meli, E., & Rindi, A. (2021). Prediction of wheel wear using innovative flexible vehicle-track interaction models. The Second International Conference on Rail Transportation (ICRT 2021).
[35] Zhai, W., Liu, P., Lin, J., & Wang, K. (2015). Experimental investigation on vibration behaviour of a CRH train at speed of 350 km/h. International Journal of Rail Transportation, 3(1), 1-16.